Metal-Ligand Tautomerism, Electron-Transfer, and C(sp^3)-H Activation by a 4-Pyridinyl-Pincer Iridium Hydride Complex

Tariq M. Bhatti, Akshai Kumar, Ashish Parihar, Thomas J. Emge, Faraj Hasanayn*, Alan S. Goldman*

*Email: fh19@aub.edu.lb; alan.goldman@rutgers.edu

Abstract

The para-N-pyridyl-based PCP pincer ligand 3,5-bis(di-*tert*-butylphosphinomethyl)-2,6-dimethylpyridine (pN-^{tBu}PCP-H) was synthesized and metalated to give the iridium complex (pN-^{tBu}PCP)IrHCl (**2-H**). In marked contrast with its phenyl-based congeners (^{tBu}PCP)IrHCl and derivatives, **2-H** is highly air sensitive and reacts with oxidants such as ferrocenium, trityl cation, and benzoquinone. These oxidations ultimately lead to intramolecular activation of a phosphino-t-butyl C(sp^3)-H bond and cyclometalation. Considering the greater electronegativity of N than C, **2-H** is expected to be less easily oxidized than simple PCP derivatives; DFT calculations of direct one-electron oxidations are in good agreement with this expectation. However, **2-H** is calculated to undergo metal-ligand-proton tautomerism (MLPT) to give an N-protonated complex that can be described with resonance forms representing a zwitterionic complex (negative charge on Ir) and a p-N-pyridylidene (remote NHC) Ir(I) complex. One-electron oxidation of this tautomer is calculated to be dramatically more favorable than direct oxidation of **2-H** ($\Delta\Delta G°$ = 31.3 kcal/mol). The resulting Ir(II) oxidation product is easily deprotonated to give metalloradical **2•** which is observed by NMR spectroscopy. **2•** can be further oxidized to give cationic Ir(III) complex**,** $\mathbf{2^+}$, which can oxidatively add a phosphino-*t*-butyl C-H bond, and undergo deprotonation to give the observed cyclometalated product. DFT calculations indicate that less sterically hindered complexes would preferentially undergo intermolecular addition of C(sp^3)-H bonds, for example, of n-alkanes. The resulting iridium alkyl complexes could undergo facile β-H elimination to afford olefin, thereby completing a catalytic cycle for alkane dehydrogenation that is driven by one-electron oxidation and deprotonation, enabled by MLPT.

1. INTRODUCTION

Organometallic pyridinyl and pyridylidene ligands (Scheme 1) are a rich platform for multifunctional and non-innocent reactivity. Pincer ligands are privileged scaffolds in organometallic chemistry, with a wide variety of catalytic applications. Both emerged in the 1970s[1-2], and while neither took inspiration from nature at the time, the discovery of a pyridylidene-pincer nickel cofactor in lactate racemase is a gratifying example of their merger in recent years.[3-4]

Scheme 1. Pyridinyl and Pyridylidene Metal Complexes (Illustrated for Metalation at the 4- position)

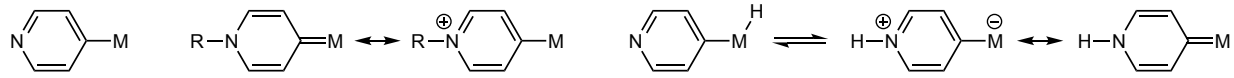

4-pyridinyl-M (or 4-pyridyl-M) | 4-pyridylidene-M (R = H, alkyl, etc.) (resonance forms) | 4-pyridinyl-MH | 4-pyridylidene-M tautomer (MLPT) (resonance forms)

Pyridinyl and especially pyridylidene ligands can be viewed as a class of Fischer carbenes[2, 5-12] in which p(π) electrons of the pyridyl nitrogen and the backbonding d-electrons of the metal compete to populate a vacant p orbital on the ipso carbon.[13] The remote nitrogen therefore strongly influences the electronics at the metal center, enabling electronic switchability and proton-responsiveness.[14-15] Quaternizing the nitrogen results in a significant increase of positive charge at the metal center, including examples with "P(C-pyridinyl)P"-pincer complexes.[16-17] Milstein and co-workers have studied P(C-pyridinyl)P-pincer ruthenium complexes as platforms for metal-ligand cooperative aromatization/dearomatization, enabling diverse reactivity including dihydrogen activation, alcohol dehydrogenation, and alcohol-amine dehydrogenative coupling.[18]

In the case of lactate racemase, mechanistic studies of the enzyme[19-20] and synthetic model complexes[21-23] have arrived at a proton-coupled hydride transfer mechanism[24] for the racemization of lactate. Current evidence points to the transfer of hydride to and from the carbenic ipso carbon.

The influence of the metal upon pyridinyl ligands is demonstrated in the markedly enhanced basicity and nucleophilicity of 2-pyridinyl and 4-pyridinyl organometallic complexes compared with free pyridine,[25-28] presumably a consequence of π-electron donation from the metal center. In the case of a metal hydride complex, this interaction would also be expected to increase its acidity. The combination of increased acidity of the hydride and high basicity at nitrogen raises the possibility of an interesting example of metal-ligand proton tautomerism (MLPT), a phenomenon which has achieved increasing recognition of late.[29-31] In this case a metal hydride would interconvert with a lower oxidation state pyridylidene tautomer - alternatively formulated as a zwitterionic pyridyl complex with a formal negative charge on the metal (Scheme 1).

Beyond the pincer motif, there are a growing number of organometallic pyridinyl and pyridylidene complexes in the literature.[5, 12] However there are no examples that include transition metal hydrides—or at least ones where the transition metal hydride is the dominant tautomer at equilibrium (examples of C-H activation alpha to a pyridyl nitrogen invariably prefer the pyridylidene tautomer at equilibrium[32-38]).

In the present study, we find that metal-ligand proton tautomerism in a 4-lutidinyl pincer iridium hydride is apparently responsible for a strong cathodic shift in its oxidation potential. A facile oxidation, in turn, initiates secondary proton- and electron-transfers, affording an unusual and highly reactive four-coordinate Ir(III) complex. Ultimately an intramolecular C(sp^3)-H activation results, driven by proton- and electron-transfer, having been initiated by MLPT.

2. EXPERIMENTAL RESULTS

2.1. Synthesis and characterization of 2-H. The 4-lutidinyl "PCP" proligand, pN-^{tBu}PCP-H (**1**), is prepared from the Hantzsch pyridine ethyl ester[39], as depicted in Scheme 2 and in the Supporting Information. X-ray quality crystals of ligand **1** were grown by slow evaporation from benzene; the crystallographically determined molecular structure is shown in Figure 1a. Refluxing a mixture of **1** with $[Ir(COD)Cl]_2$ (COD = 1,5-cyclooctadiene) in toluene under 1 atm hydrogen resulted in a change of the solution color from orange to cherry red within a few minutes, with metalation apparently complete within 30 minutes. Evaporation of solvent under vacuum afforded an orange, microcrystalline, air-sensitive powder, **2-H** (Scheme 2). ^{1}H, ^{13}C, and ^{31}P NMR spectra of **2-H** are similar to those of (^{tBu}PCP)IrHCl (**3-H**),[1, 40] (*p*-NO_2-^{tBu}PCP)IrHCl,[41] (*p*-MeO-^{tBu}PCP)IrHCl,[42] and (*p*-Me_2N-^{tBu}PCP)IrHCl.[43] In benzene-d_6, a hydride resonance appears as a triplet at -41.9 ppm ($^2J_{P\text{-}H}$ = 12 Hz) in the ^{1}H NMR spectrum. The phosphino-*t*-butyl groups as well as the methylene protons of the pincer arms are inequivalent in the ^{1}H NMR spectrum; the *t*-butyl groups appear as two virtual triplets and the methylene protons appear as two doublets of virtual triplets. The selectively proton-decoupled ^{31}P NMR spectrum shows a doublet at 68.8 ppm with a coupling to the hydride proton of $^2J_{P\text{-}H}$ = 12 Hz. X-ray quality crystals of complex **2-H** were grown from pentane/toluene at -40 °C and the XRD structure (Figure 1b) was consistent with the assignment based on NMR spectroscopy, although the hydride ligand was not unambiguously located.

Scheme 2. Synthesis of pN-^{tBu}PCP-H (1) and Metalation to give 2-H

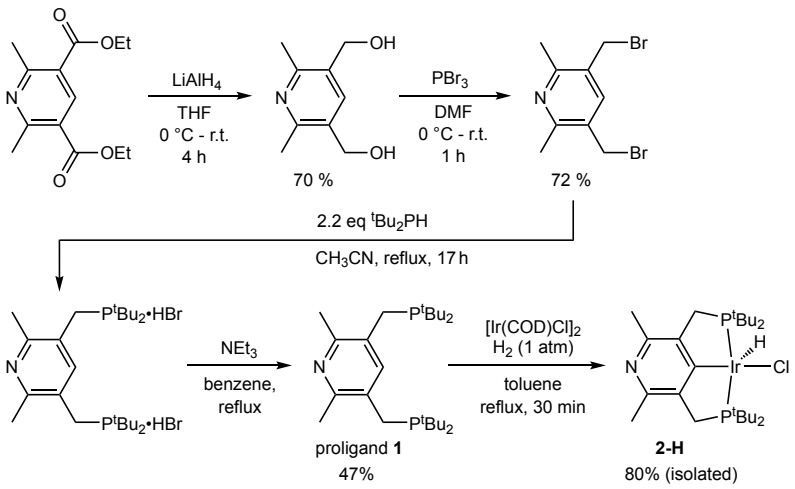

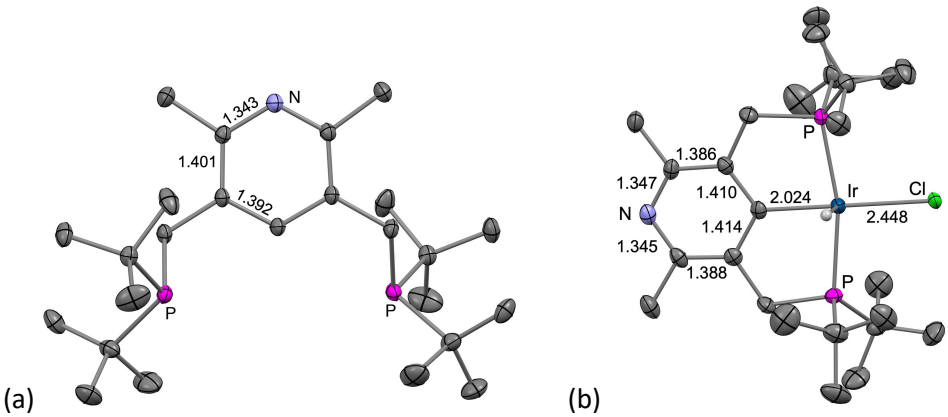

Figure 1. Molecular structures of (a) (pN-^{tBu}PCP-H) (**1**) and (b) (pN-^{tBu}PCP)IrHCl (**2-H**) determined by XRD. Hydrogen atoms, except for the hydride ligand, omitted for clarity. Selected bond lengths in Å.

2.2. Basicity of 2-H. To estimate the basicity of the remote nitrogen in complex **2-H** a solution of 2,6-lutidinium chloride in DMSO (pK_a 4.46) is added to solid **2-H** (which is insoluble in DMSO). **2-H** was completely taken up into solution—indicating that the remote nitrogen was protonated by the 2,6-lutidinium salt. The resulting **2-H•HCl** is soluble in DMSO and water. However, when a solution of DBU•HCl in DMSO (pK_a = 13.9 in DMSO[44]) is added to solid **2**, only some of the material is taken into solution, suggesting that the pK_a of **2-H•HCl** is perhaps similar to that of DBU•HCl. Determination of the protonation equilibrium is confounded, however, by the heterogeneous nature of this reaction as well as possible coordination of solvent or chloride trans to the hydride in **2-H•HCl.** Computationally, using Density Functional Theory (see details below and Supporting Information), the pyridinyl nitrogen of **2-H** is predicted to be 3.6 pK_a units more basic (in DMSO) than the corresponding nitrogen of **1** (Scheme 3).

Scheme 3. Calculated equilibrium illustrating increased basicity of **1** upon metalation

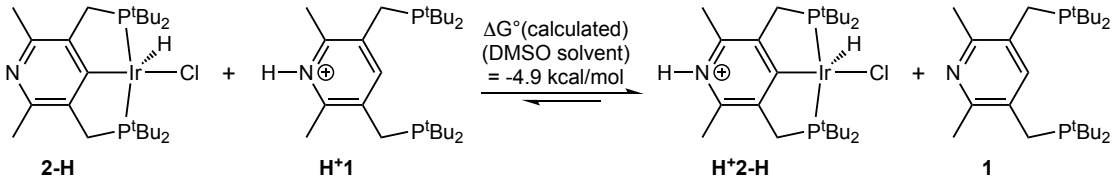

2.3. Oxidations of 2-H. Orange-red solutions of complex **2-H** in non-coordinating solvents immediately turn dark purple upon exposure to air. This attracted our interest because the analogous "parent" complex bearing a phenyl-based PCP ligand, (^{tBu}PCP)IrHCl (**3-H**), and even analogs bearing π-donating para-substituents (methoxy[42] or dimethylamino[43]) do not show similar air-sensitivity. We therefore investigated the oxidation of **2-H** with oxidants that generally afford simpler reactivity than O_2. Importantly, and consistent with the pronounced difference in air-sensitivity between **2-H** and **3-H**, those oxidants described below that are found to react rapidly with **2-H** undergo no reaction with **3-H** under the same conditions in the timeframe of the investigation.

Table 1. Reaction of 2-H with Various Oxidants

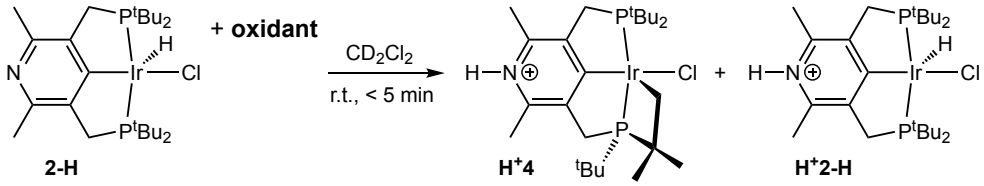

Entry	$[2\text{-}H]_0$	Oxidant	Base	$[H^+4]$ (mM)	$[H^+2\text{-}H]$ (mM)
1	17.4 mM	$[Cp_2Fe^+][PF_6^-]$ (1 eq)[a]	-	7.2	8.3
2	14.3 mM	$[Cp_2Fe^+][PF_6^-]$ (2 eq)	-	8.8	5.5
3	11.7 mM	$[Cp_2Fe^+][PF_6^-]$ (2 eq)	2,6-lutidine (9 eq)	10.6	-
4	12.5 mM	$[Ph_3C^+][B(C_6F_5)_4^-]$ (1 eq)	-	4.9	7.6
5	7.5 mM	$[(p\text{-}MeOC_6H_4)Ph_2C^+][BF_4^-]$ (2 eq)	-	*No reaction*	
6	11.1 mM	$[Cp^*_2Fe^+][BF_4^-]$ (2 eq)[b]	-	*No reaction*	

a) Benzene solvent. (b) Cp* = η^5-C_5Me_5

*2.3.1. Reaction of **2-H** with Cp_2Fe^+.* When 1 equivalent of ferrocenium hexafluorophosphate is added to a solution of **2-H** in dichloromethane-d_2 the orange solution rapidly turns dark purple, followed by a slow conversion to light red. ^{31}P and ^1H NMR spectroscopy reveal that **2-H** has undergone quantitative conversion. The $^{31}P\{^1H\}$ NMR spectrum reveals the presence of two major species in an approximately 1:1 ratio (Scheme 4).

Scheme 4. Reaction of **2-H** with 1 equivalent ferrocenium hexafluorophosphate

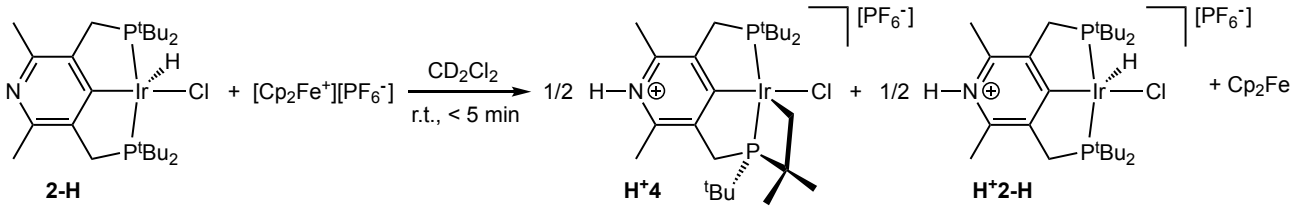

One of the two major products observed is N-protonated, **2-H** (**H^+2-H**; Scheme 4) which appears in the selectively decoupled ^{31}P NMR spectrum as a doublet at 67.9 ppm, coupled ($^2J_{P\text{-}H}$ = 11.5 Hz) to a hydride at -40.5 ppm in the ^1H NMR spectrum. The phosphino-*t*-butyl groups appear as two overlapping virtual triplets at 1.37 ppm. The second set of signals in the ^{31}P NMR spectrum comprises two doublets, at 49.8 ppm at 8.7 ppm, with a strong mutual coupling of 345 Hz. ^{31}P-^1H HMBC (see Supporting Information) was used to correlate the ^{31}P NMR signal at 8.7 ppm with two doublets in the ^1H NMR spectrum at 1.59 ppm and 0.88 ppm, each with integral 3, as well as with two broad apparent triplets at

1.67 and 3.30 ppm, each with integral 1 (attributable to the two methyl groups and the two methylene protons, respectively, of the cyclometalated *t*-butyl group). The doublet at 49.8 ppm in the ^{31}P NMR spectrum correlates with two doublets in the ^{1}H NMR spectrum, each with integral 9, at 1.31 ppm and 1.19 ppm. The presence of two overlapping signals at 10.66 ppm and 10.57 ppm in a near 1:1 ratio in the ^{1}H NMR spectrum indicated the new products are both protonated at the pyridinyl nitrogen. These spectral features are characteristic of a cyclometalated pincer complex,[42-49] in which one of the *t*-butyl groups of **2-H** has undergone C-H activation to form **H$^+$4** (Scheme 4). Thus, coupled with two one-electron oxidations and Ir-C bond formation, the hydride proton and a *t*-butyl proton of **2-H** have undergone net transfer to the pyridinyl nitrogen atoms of the now-cyclometalated complex **4** and another molecule of **2-H**.

Addition of *two* equivalents ferrocenium hexafluorophosphate to a solution of **2-H** in dichloromethane-d_2 also results in the orange solution rapidly turning dark purple followed by slow conversion to red, and ^{31}P and ^{1}H NMR spectroscopy again reveal that **2-H** has undergone quantitative conversion. The ratio of **H$^+$4** to **H$^+$2-H** in this case is ca. 1.6:1, in contrast with the ratio of ca. 1:1 obtained from the reaction with 1 equiv $[Cp_2Fe][PF_6]$ (Scheme 4). It appears that, while in this case there are enough oxidizing equivalents to convert all **2-H** to **H$^+$4**, the protonation of all pN-pyridyl-PCP nitrogens upon reaction with one equiv $[Cp_2Fe][PF_6]$ (Scheme 4) strongly inhibits further oxidation. Consistent with this hypothesis, in the presence of excess 2,6-lutidine (9 equiv), the reaction of two equiv $[Cp_2Fe][PF_6]$ with **2-H** results in nearly complete (90%) conversion to **H$^+$4** upon mixing (Scheme 5).

Scheme 5. Reaction of **2-H** with 2 equivalents ferrocenium hexafluorophosphate and lutidine

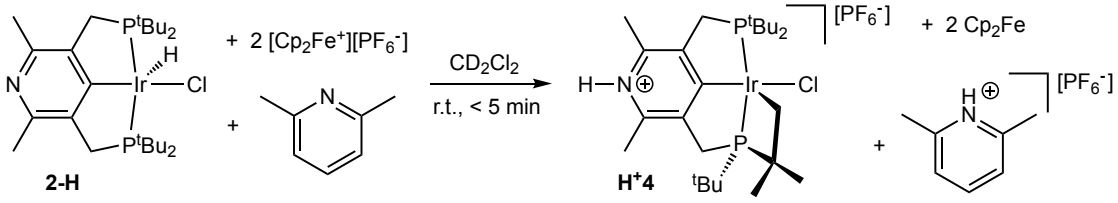

*2.3.2. Reaction of **2-H** with Ph_3C^+.* Mixing complex **2-H** with 1 equivalent of $[Ph_3C^+][B(C_6F_5)_4^-]$ (-0.11 V[50] vs. Fc/Fc^+) in dichloromethane-d_2 results in an instantaneous color change to dark purple. The solution then gradually lightens to orange. The ^{1}H NMR spectrum reveals a 0.7:1 ratio of **H$^+$4** to **H$^+$2-H**, along with a half equivalent of Gomberg's dimer ($(Ph_3C)_2$; Scheme 6). Thus the trityl cation has acted as a single-electron oxidant, yielding approximately the same results as were obtained with 1 equivalent $[Cp_2Fe^+][PF_6]$.

Scheme 6. Reaction of **2** with 1 equivalent $[Ph_3C^+][B(C_6F_5)_4^-]$

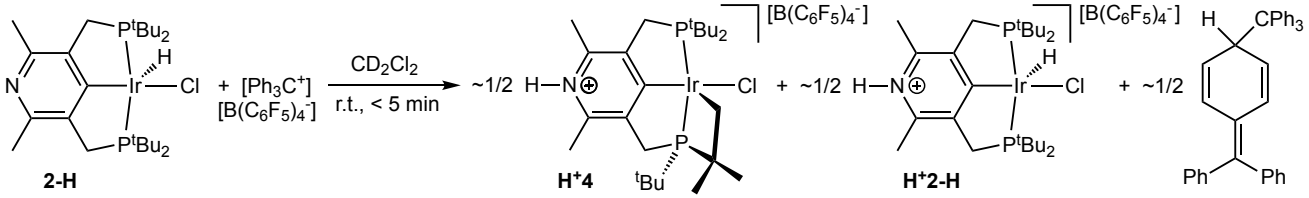

*2.3.3. Reactions of **2-H** with benzoquinone (BQ).* The reaction of complex **2-H** with one equivalent of BQ leads to quantitative conversion to **4** and hydroquinone within 48 hours at 22 °C (Scheme 7). Hydroquinone precipitates as a white solid from the reaction mixture. Following filtration, slow evaporation of the filtrate at ambient temperature produced crystals of complex **4**, the molecular structure of which was determined by XRD (Figure 2).

Scheme 7. Reaction of **2** with 1 equivalent benzoquinone

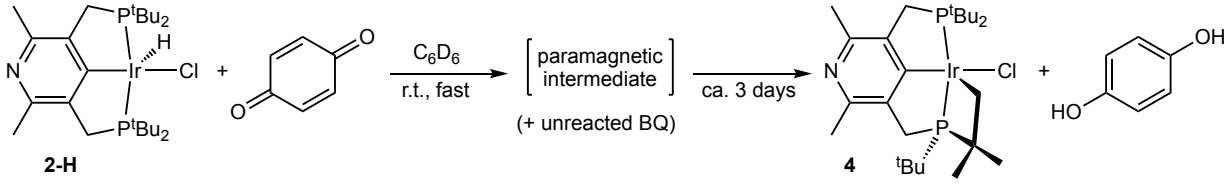

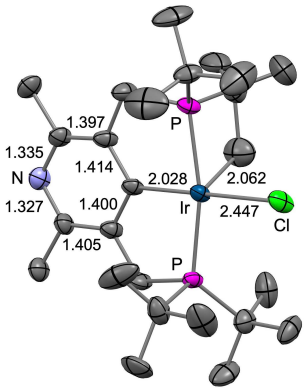

Figure 2. Molecular structure of **4** determined by XRD. H atoms omitted for clarity. Selected bond lengths in Å.

A paramagnetic intermediate is observed in the course of the reaction of **2-H** with BQ**.** Monitoring the oxidation of **2-H** (7 mM) by 540 mM BQ in benzene-d_6 reveals, within 2 minutes of mixing, that approximately 50% of the starting material **2** has been converted to this paramagnetic species which has broad signals at δ -31 and δ 14.8 in the ^{1}H NMR spectrum that integrate in a 1:6 ratio. This ratio allows assignment of the signals to the α-methyl groups and *t*-butyl groups respectively. It follows, then that this intermediate contains two mirror planes of symmetry, which renders all four *t*-butyl groups as well as the two α-methyl groups equivalent on the relevant NMR timescale. The methylene signals of the

pincer arms in this paramagnetic intermediate were not observed, and may be broadened into the baseline. The signals of the intermediate diminish, with concomitant growth of signals attributable to **4** over the next 2 hours (see Supporting Information).

2.3.4. Characterization of the paramagnetic intermediate resulting from the initial single-electron oxidations. In an effort to characterize the paramagnetic intermediate, a solution of **2-H** (12 mM) in benzene-d_6 was allowed to react with only a slight excess (1.5 eq) of benzoquinone for 5 minutes at 25 °C; 29% conversion of **2-H** to the paramagnetic intermediate is observed by ^{1}H NMR. A 4-fold excess of TEMPO-H (1-hydroxy-2,2,6,6-tetramethyl-piperidine)(BDFE = 65.2 kcal/mol[51]) was then added to quench the paramagnetic species. The ^{1}H NMR spectrum taken immediately afterward indicated that **2-H** was the sole remaining iridium-containing species in solution (Scheme 8). On the basis of these data, the paramagnetic species **2•** is assigned as the square planar product resulting from loss of H from **2-H**.

Scheme 8. Reaction of **2•**, generated in situ, with TEMPO-H, to give **2-H**

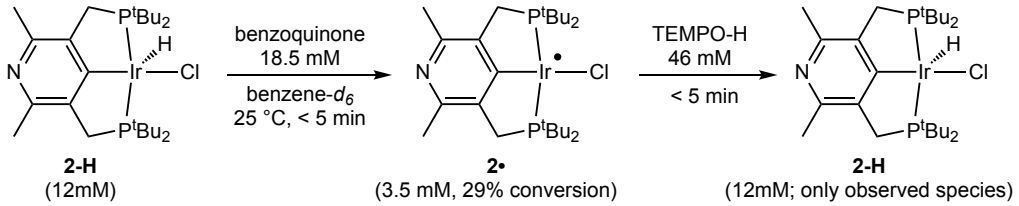

In accord with our assignment of **2•**, it was independently generated by the reaction of **2-H** with the isolable tri-t-butylphenoxy radical[51-53] (BDFE = 76.7 kcal/mol[51-52])(20% yield and conversion by 1H NMR; Scheme 9).

Scheme 9. Reaction of **2-H** with 2,4,6-^{t}Bu$_3$C$_6$H$_3$O•

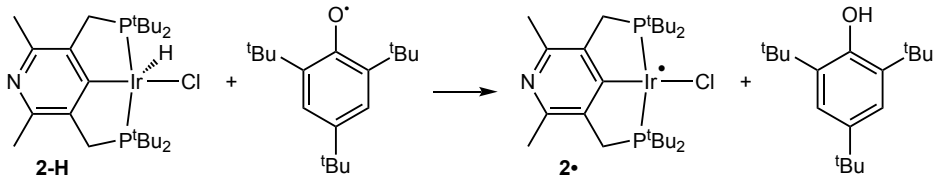

3. MECHANISTIC CONSIDERATIONS AND DFT CALCULATIONS

3.1. Initial oxidation of 2-H via MLPT. Based on the greater electronegativity of N than C, simple one-electron oxidation of **2-H** is expected to be thermodynamically less favorable than oxidation of phenyl-based (^{tBu}PCP)IrHCl (**3-H**) or its 3,5-dimethylphenyl-based derivative **3'-H** (which is even more closely analogous to **2-H**). The results of DFT calculations are consistent with this simple reasoning: the ionization energy of **2-H** is calculated to be 5.2 kcal/mol less favorable than of **3'-H**. In absolute terms, one-electron oxidation of **2-H** by Cp_2Fe^+ in CH_2Cl_2 is calculated to be endergonic by 14.0 kcal/mol. However, we calculate that **2-H** can undergo transfer of H from Ir to the pyridinyl nitrogen; the resulting

MLPT tautomer, **2-H-t**, is 6.5 kcal/mol higher in free energy than **2-H**. As shown in Figure 3 (top), there are two limiting resonance structures for the tautomer **2-H-t**, one representing a zwitterionic form (**2-H-t$_{zwit}$**) and one a carbene form (**2-H-t$_{carb}$**). A computed significant contraction of the Ir-C bond length (1.94 Å vs. 2.03 Å for **2-H**), and a more pronounced alternation of interatomic distance in the heterocyclic ring of **2-H-t** compared with that of **2-H**, implicates significant contribution from resonance form **2-H-t$_{carb}$** (Figure 3).

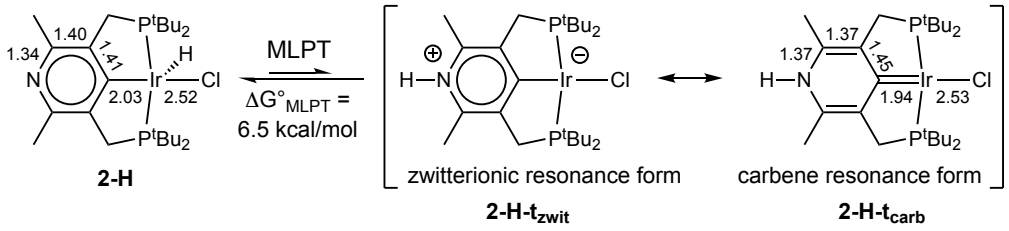

2-H zwitterionic resonance form carbene resonance form

2-H-t$_{zwit}$ **2-H-t$_{carb}$**

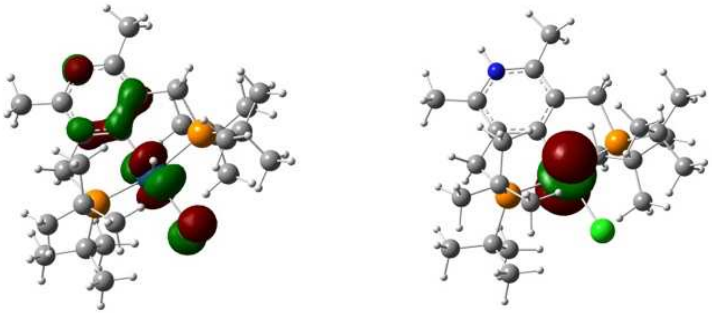

HOMO of **2-H** (-4.7 eV) HOMO of **2-H-t** (-3.7 eV)

Figure 3. DFT-calculated structures and HOMOs of **2-H** and **2-H-t**. Bond lengths in Å.

One plausible pathway for the proposed MLPT would be via initial intermolecular proton transfer of the Ir-H proton of **2-H** to the nitrogen of a second **2-H** molecule. The barrier for this step is computed to be quite low (15.6 kcal/mol, Figure 4). Proton transfer initially gives an ion-pair that can rearrange to deliver the proton to the nitrogen site of the deprotonated molecule of **2-H**, thereby affording **2-H-t.**

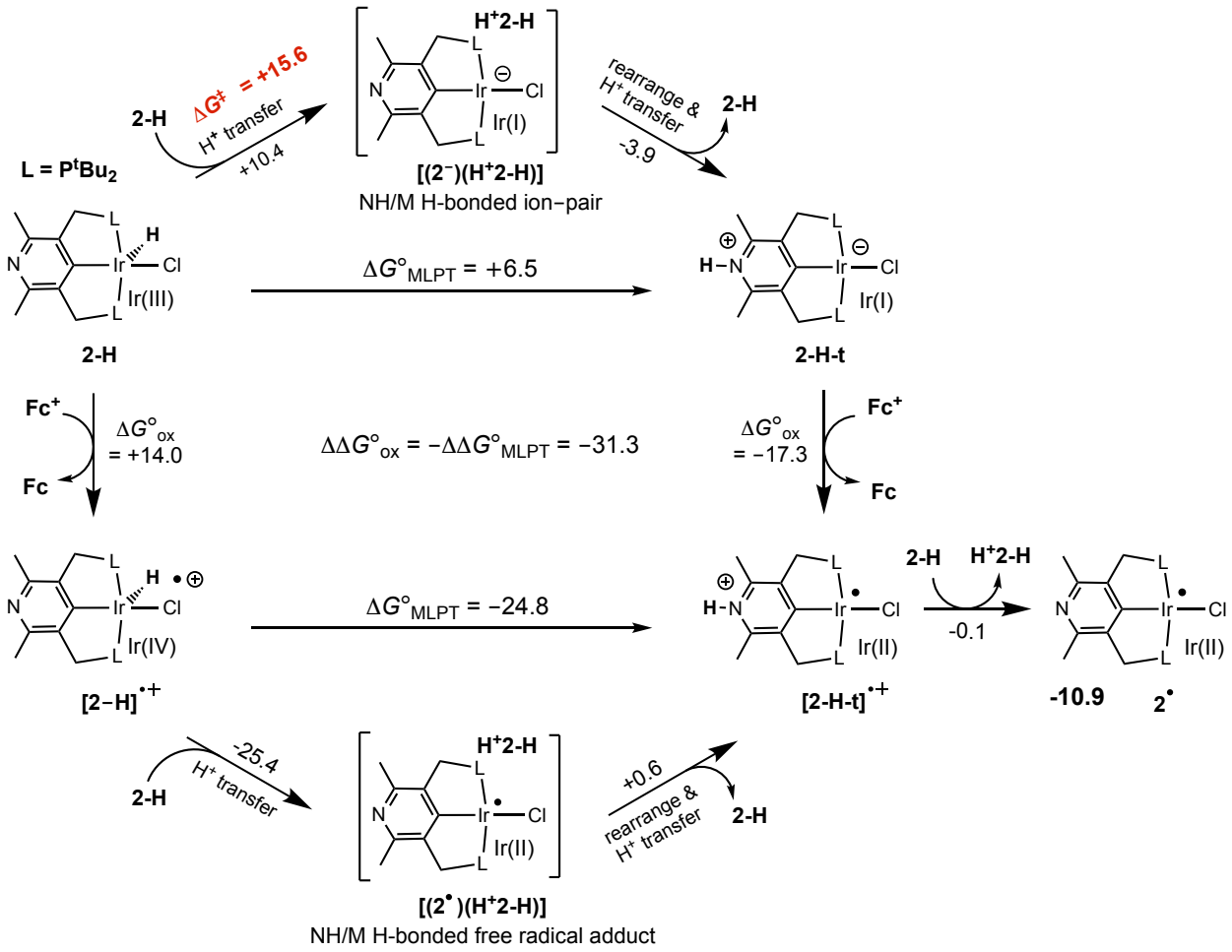

Figure 4. Oxidation of **2-H**, directly or via tautomer **2-H-t**, by Cp_2Fe^+ (**Fc**$^+$) and subsequent deprotonation by another molecule of **2-H**. Calculated Gibbs free energies at 298 K and 1 M in kcal/mol; M06L-D3 in CH_2Cl_2 continuum.

While tautomerization of **2-H** to give **2-H-t** is endergonic by only 6.5 kcal/mol, the oxidation of **2-H-t** by Cp_2Fe^+ is calculated to be very favorable (ΔG°_{ox} = -17.3 kcal/mol). Thus MLPT of **2-H** favors oxidation by a remarkable extent of 31.5 kcal/mol ($\Delta\Delta G^\circ_{ox}$, Figure 4). For purposes of qualitatively understanding this effect, it is perhaps convenient to consider the zwitterionic resonance form **2-H-t$_{zwit}$**. The parent complex **2-H** has a d^6 Ir(III) center and a HOMO derived largely from the metal 5d$_{xz}$ orbital (Figure 3). MLPT to give **2-H-t$_{zwit}$** creates a square planar complex with a d^8 Ir(I) center having a formally negative charge and a 5d$_{z2}$ HOMO that is 1.0 eV higher than the HOMO in **2-H** (Fig. 3). The reductive nature of MLPT with respect to the metal thereby explains the greatly more favorable oxidation of **2-H-t** relative to **2-H.**

Note that the difference in the oxidation energies of **2-H** and **2-H-t** ($\Delta\Delta G^\circ_{ox}$ = -31.3 kcal/mol) is necessarily equal to the difference in the tautomerization energies of **2-H** and its oxidized form [**2-H**]$^{\bullet+}$ ($-\Delta\Delta G^\circ_{MLPT}$). Thus, in contrast with the parent complex **2-H**, MLPT of the radical cation **[2-H]**$^{\bullet+}$ is highly exergonic (ΔG°_{MLPT} = -24.8 kcal/mol; Figure 4). This may be viewed in terms of the increased metal

oxidation state and the increased electric charge greatly increasing the acidity of the IrH bond in **[2-H]$^{\bullet+}$** relative to **2-H** (with an expected decrease of at least 15 pK_a units[54-55]), but having a much smaller effect on the basicity of the nitrogen which is distant from the center of oxidation. Thus, upon oxidation, the nitrogen becomes the favored site for the proton.

For a given molecule, $\Delta G°_{MLPT}$ is equal to the difference between the Ir-H and N-H BDFEs. Similar to the acidity, the N-H BDFE in **2-H-t** is not expected to greatly change upon oxidation. Thus the large change in $\Delta G°_{MLPT}$ implies that the BDFE of the Ir-H bond in **2-H** is greatly weakened upon oxidation.

Oxidation of **2-H-t** generates the free radical cation **2-H-t$^{\bullet+}$**. Subsequent deprotonation of **2-H-t$^{\bullet+}$** by an unreacted molecule of **2-H** is computed to be essentially ergoneutral ($\Delta G°$ = 0.1 kcal/mol), yielding the d^7 Ir(II) complex **2$^{\bullet}$**, our assignment for the paramagnetic intermediate observed in the reaction with benzoquinone (Schemes 7 and 8). The net energy of formation of **2•** and **H$^+$2-H** from two molecules of **2-H** and ferrocenium is computed to be quite negative, $\Delta G°$ = -10.9 kcal/mol. MLPT thereby enables a facile path for net "H-abstraction" from a metal-hydride, **2-H**, via one-electron oxidation. The calculations in the next section show that oxidation of **2$^{\bullet}$** by another ferrocenium is viable, and that it triggers intramolecular C-H activation.

3.2. Oxidation of 2$^{\bullet}$ and intramolecular C-H activation. Oxidation of the Ir(II) complex **2$^{\bullet}$** by a second equivalent of ferrocenium is calculated to be only slightly endergonic ($\Delta G°$ = 7.9 kcal/mol). We calculated two minima, with nearly identical energies, for the resulting four-coordinate d^6 cation. One of these has a square planar geometry with a triplet spin state (^{3}**2$^+$**), while the other has a seesaw geometry with a closed shell singlet state (**2$^+_{bent}$**). **2$^+_{bent}$** features an agostic C-H bond from a phosphino-*t*-butyl group donating into the otherwise empty orbital of the metal, with Ir-H and Ir-C bond distances of 2.08 and 2.81 Å[56]. No minimum with an agostic bond could be located for the triplet state, which is not surprising given that this state has no empty metal d atomic orbital.

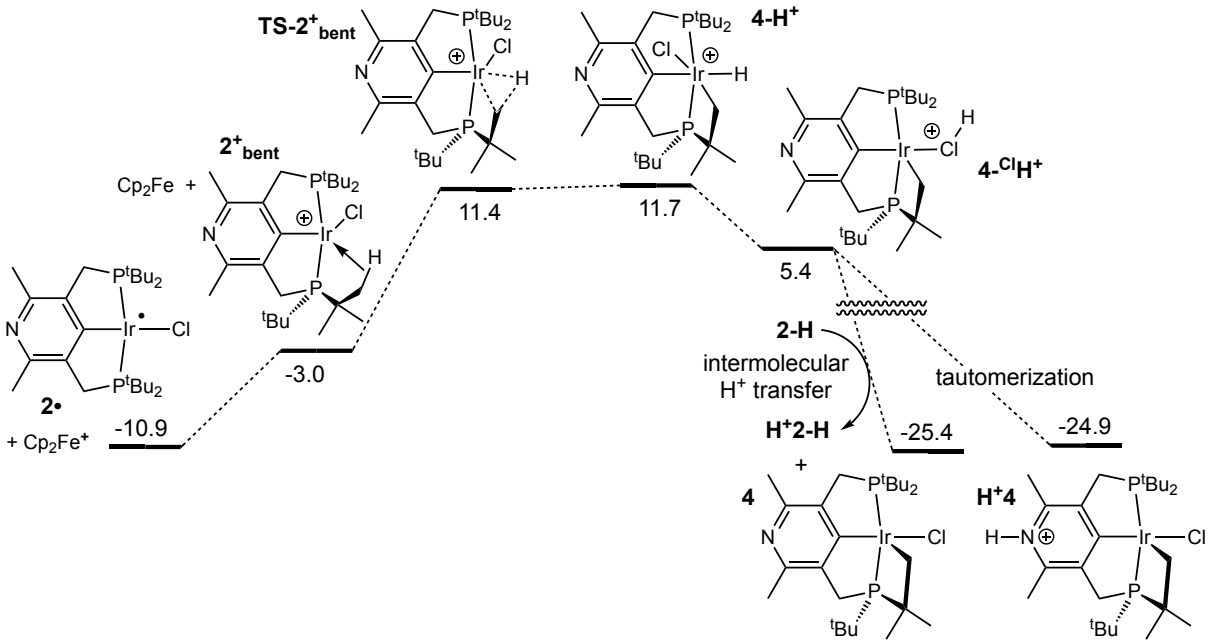

Figure 5. Oxidation of **2•** by Cp_2Fe^+, and subsequent cyclometalation and deprotonation to give **4**; calculated free energies in kcal/mol normalized relative to two **2-H** and Cp_2Fe^+ (Figure 4); M06L-D3 in CH_2Cl_2 continuum.

Oxidative addition of the agostic C-H bond of $\mathbf{2^+_{bent}}$ is computed to proceed readily ($\Delta G^‡$ = 14.4 kcal/mol). The transition state $\mathbf{TS\text{-}2^+_{bent}}$ has a geometry characterized by near complete C-H bond cleavage (1.65 Å) and large degree of Ir-H (1.56 Å) and Ir-C (2.22 Å) bond formation. $\mathbf{TS\text{-}2^+_{bent}}$ leads to the six-coordinate cyclometalated $\mathbf{4\text{-}H^+}$ which is calculated to be extremely acidic. Proton transfer from $\mathbf{4\text{-}H^+}$ to the pyridinyl nitrogen of a second, neutral, molecule of **2-H**, to afford the observed metallacycle product **4** is highly exergonic ($\Delta G°$ = -36.6 kcal/mol). However, the proton in $\mathbf{4\text{-}H^+}$ is in a sterically very encumbered environment and may be kinetically inaccessible for direct transfer to a pyridinyl nitrogen. A proton shift from the iridium center in $\mathbf{4\text{-}H^+}$ to a phosphino group (bridging an Ir-P bond [57-59]) is exergonic by 4.3 kcal/mol, and the proton on the phosphine in $\mathbf{4\text{-}^PH^+}$ should be more accessible for transfer to **2-H**. Similarly, a proton shift from the metal in $\mathbf{4\text{-}H^+}$ to the chloride ligand (Figure 5) is also exergonic, by 6.3 kcal/mol, and leads to an HCl molecule loosely coordinated to an unsaturated cationic species ($\mathbf{4\text{-}^{Cl}H^+}$). This species could readily transfer a proton to the basic nitrogen site of a molecule of **2-H**, either directly or perhaps by initial dissociation of free HCl. Attempts to locate TSs for these or other metal-to-ligand proton shifts were not successful due to very flat PESs but it seems clear that the very favorable intermolecular deprotonation of $\mathbf{4\text{-}H^+}$ would occur readily via one or more of these or perhaps other pathways.

4. CONSIDERATIONS OF SELECTIVITY AND IMPLICATIONS FOR CATALYSIS

As discussed above, unlike the unsubstituted parent pincer complex (^{tBu}PCP)IrHCl,[60] **3-H**, or derivatives, the para-pyridyl-based **2-H** reacts rapidly at ambient temperature with oxidants including O_2, trityl cation, ferrocenium, and benzoquinone. We attribute the facile oxidation of **2-H** to a preceding MLPT reaction. The equilibrium of the MLPT reaction lies toward **2-H** rather than **2-H-t**. This stands in contrast to 2-pyridinyl[61-62] and imidazolyl metal hydride complexes[32-33, 36] where proton transfer from metal to ligand is favored at equilibrium. Recently, Kuo and Goldberg have reported an iridium pincer system, based on a bis(pyrazolyl)pyridine ligand, in which both Ir(III)-H and (L-H)Ir(I) tautomers are observable.[29] But while formation of **2-H-t** is calculated to be slightly endergonic ($\Delta G°$ = 6.5 kcal/mol), DFT calculations predict that its oxidation is far more favorable than that of **2-H** (by 31.3 kcal/mol), to give $\mathbf{H^+2^•}$ which is then deprotonated to give $\mathbf{2^•}$. Oxidation of the resulting Ir(II) complex $\mathbf{2^•}$ is calculated to yield intermediate, $\mathbf{2^+_{bent}}$, which is calculated to readily insert into an sp^3 C-H bond of a phosphino-*t*-butyl group to produce the highly acidic species $\mathbf{4\text{-}H^+}$, which upon deprotonation gives the observed cyclometalated complex **4.**

It is possible that cationic, d^6 pincer-iridium complexes similar to $\mathbf{2^+_{bent}}$ have been involved in prior examples of cyclometallation reactions without being identified. For example, Koridze and coworkers reported that treatment of (^{tBu}POCOP)IrHCl and (EtO_2C-^{tBu}POCOP)IrHCl with trifluoroacetic acid leads to

cyclometallation with loss of H_2.[48] Mayer and coworkers undertook cyclic voltammetry studies of (^{tBu}PCP)IrHCl and (MeO-^{tBu}PCP)IrHCl, in which they found that oxidation leads to cyclometallation with loss of H_2.[42, 63-64] They proposed that upon one-electron oxidation, cyclometalation to yield H_2 (Scheme 10, eq b) becomes thermodynamically favorable. Our calculations, however, strongly indicate that the thermodynamics of such dehydrogenative cyclometalation reactions are substantially endergonic and strikingly unaffected by single-electron oxidation (Scheme 10).

Scheme 10. Thermodynamics of dehydrogenative cyclometalation of (X-^{tBu}PCP)IrHCl and of their corresponding one-electron oxidation products

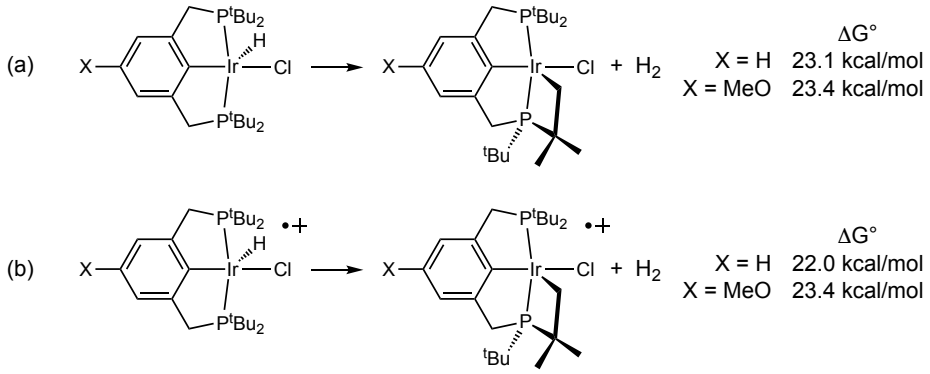

It is important to note that [(pN-^{tBu}PCP)Ir^{III}Cl$^+$], **2**$^+$, undergoes *intra*molecular C-H activation, in contrast with Ir(I) complexes of isostructural ^{tBu}PCP or ^{tBu}POCOP ligands which are among the most well-known complexes for *inter*molecular C-H activation (and functionalization)[65-67]. The different reactivity is undoubtedly not based on electronic factors; the C-H bond of a *t*-butyl group is certainly not very different than that of an *n*-alkane, with respect to electronic factors, in any way that would strongly bias its relative reactivity toward an Ir(III) versus an Ir(I) center. Presumably the preference of the Ir(III) species to undergo intramolecular C-H addition, in contrast with the Ir(I) fragments, is based on the very different geometries and steric environments of the respective vacant coordination sites that enable the C-H addition reactions. Specifically, the active site in the case of (pincer)Ir(I) complexes is trans to the pincer aryl carbon, as compared to a site cis to the analogous carbon in the case of [(pN-^{tBu}PCP)Ir^{III}Cl$^+$]. The trans site of (PCP)Ir(I) complexes is significantly less crowded than the cis sites[68], allowing intermolecular access of an alkane. Conversely, the coordination site cis to the pincer ipso carbon is easily accessible to a phosphino-*t*-butyl group while cyclometalation, in contrast with intermolecular C-H activation (in this case or generally[69-70]), is not disfavored by crowding.

Calculations were conducted with the parent fragment (^{tBu}PCP)IrCl (**3**) to explore and quantify the proposed role of steric factors and the ligand architecture. Cyclometalation by **3**$^+$ (coupled with deprotonation by triethylamine as a model base) is found to be 9.5 kcal/mol more exergonic than addition of a propane primary bond[71-72], while the barrier to cyclometalation, $\Delta G^{\ddagger}$, is also (somewhat coincidentally) 9.5 kcal/mol less (Figure 6). In contrast, for the less crowded di-isopropyl-phosphino analogue, (^{iPr}PCP)IrCl$^+$, cyclometalation is calculated to have a barrier very slightly *greater* ($\Delta\Delta G^{\ddagger}$ = 0.3

kcal/mol) than the barrier to addition of a propane primary bond (which is calculated to be quite low, $\Delta G^{\ddagger}$ = 14.6 kcal/mol). Thus, in comparing [(^{tBu}PCP)IrCl^{+}] versus [(^{iPr}PCP)IrCl^{+}], the calculated difference in selectivity for intermolecular versus intramolecular C-H activation is quite pronounced, 9.8 kcal/mol (expressed as $\Delta\Delta\Delta G^{\ddagger}$; Figure 6). The thermodynamic preference for cyclometalation by **3**$^{+}$ versus intermolecular C-H addition is also much greater than for (^{iPr}PCP)IrCl^{+}, $\Delta\Delta G°$ = -9.5 kcal/mol versus -1.9 kcal/mol ($\Delta\Delta\Delta G°$ = 7.6 kcal/mol).

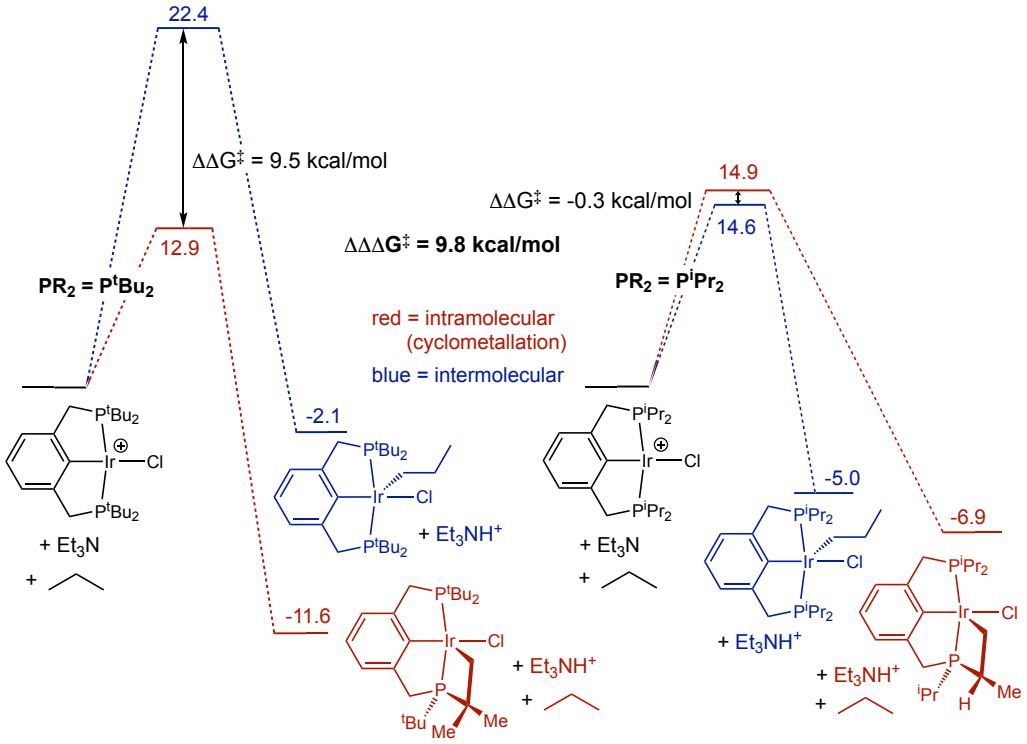

Figure 6. Free energies (kcal/mol) of intramolecular (cyclometalation) versus intermolecular C-H activation by (^{R4}PCP)IrCl^{+}; R = ^{i}Pr and ^{t}Bu; M06L-D3 in *n*-heptane continuum. (Et_3N used as a model base; the choice of base has no effect on values of $\Delta G^{\ddagger}$ or relative values of $\Delta G°$)

The reversal of selectivity in C-H activation, from intramolecular to intermolecular by the simple substitution of *i*-Pr groups for *t*-Bu groups, demonstrates that the observation of cyclometalation does not reflect an intrinsic tendency of cationic Ir(III) centers to necessarily undergo cyclometalation. This has important implications for exploiting, for catalytic applications, the unusual reactivity described in this work. For example, successive oxidations and loss of a proton from a more cyclometalation-resistant analogue of **2-H**, if followed by addition of an *n*-alkyl C-H bond would yield a species analogous to **4**, of the general form (PCP)IrCl(*n*-alkyl). β-H elimination by this 16-electron species, in analogy with the well-known behavior of (PCP)IrH(*n*-alkyl) complexes[65-67], would return the hydride reactant; in the case of (^{iPr}PCP)IrCl the calculated barrier, $\Delta G^{\ddagger}$, is a modest 17.9 kcal/mol (Scheme 11). These reactions would comprise a catalytic cycle for alkane dehydrogenation, driven by two proton-coupled electron transfers.

Scheme 11. β-H-elimination by (hypothetical) product of C-H addition/deprotonation by (^{iPr}PCP)IrCl$^+$

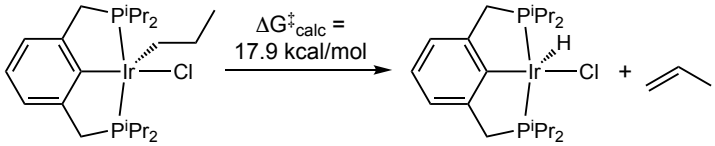

One could envision this applied in an electrochemical system or in a purely chemical system driven by O_2 as the ultimate oxidant (directly, or indirectly as in the case of the Wacker reaction system[73]). We have previously reported that (^{tBu}PCP)IrH_2 can catalyze PCET-driven alkane dehydrogenation;[74] however that catalyst operates via an Ir(I) species which is subject to over-oxidation, and thus far it requires a strong base for deprotonation. The high-oxidation-state cycle envisioned here might circumvent either or both of these issues.

5. CONCLUSIONS

(pN-^{tBu}PCP)IrHCl, **2-H**, is intrinsically more difficult to oxidize (i.e. has a higher oxidation potential or free energy of one-electron oxidation) than the phenyl-based analog (^{tBu}PCP)IrHCl or the even more closely related derivative, **3'-H**. Nevertheless, **2-H** displays much greater reactivity with oxidants including ferrocenium, trityl cation, and benzoquinone, as well as O_2.

DFT calculations reveal the key intermediacy of an Ir(I) tautomer, resulting from MLPT, which can be characterized as either a zwitterion or a remote NHC complex. This tautomer is subject to facile one-electron oxidation to give the net loss of a hydrogen atom from the iridium center. The resulting product is a cationic N-protonated iridium(II) complex **H$^+$2$^\bullet$**. Deprotonation then gives **2$^\bullet$**, which is also fairly easily oxidized, to give **2$^+$**, completing the net loss of a hydride from **2-H**. The 4-coordinate *d*^{6} iridium complex **2$^+$** is calculated to undergo cyclometalation/C-H addition to give the strongly acidic complex **4-H$^+$**. Loss of a proton from **4-H$^+$** gives the observed cyclometalated iridium(III) complex **4**.

PCP-type pincer ligands have yielded a very rich manifold of chemistry, particularly for the activation of small molecules and especially C-H bonds.[65-67] The para-pyridyl pincer ligand appears to add a new dimension to this manifold by allowing the low-energy deprotonation of the metal center of a hydride complex, via MLPT. In this work we see that such deprotonation facilitates oxidation, leading to the net loss of H• and ultimately H$^-$, to give a highly reactive coordinatively unsaturated cationic metal center.

■ ASSOCIATED CONTENT

Supporting Information

Complete experimental details and synthetic procedures, NMR data, computational details, computed energies and thermodynamic quantities (**PDF**)

Accession Codes

CCDC 2215473 - 2215475 contain the supplementary crystallographic data for this paper. These data can be obtained free of charge via www.ccdc.cam.ac.uk/ data_request/cif, or by emailing data_request@ccdc.cam.ac.uk, or by contacting The Cambridge Crystallographic Data Centre, 12 Union Road, Cambridge CB2 1EZ, UK; fax: +44 1223 336033.

■ AUTHOR INFORMATION

Corresponding Authors

Faraj Hasanayn − *Department of Chemistry, American University of Beirut, Beirut 1107 2020, Lebanon;* orcid.org/0000-0003-3308-7854; Email: fh19@aub.edu.lb

Alan S. Goldman − *Department of Chemistry and Chemical Biology, Rutgers, The State University of New Jersey, New Brunswick, New Jersey 08854, United States;* orcid.org/0000-0002-2774-710X; Email: alan.goldman@rutgers.edu

Authors

Tariq M. Bhatti − *Department of Chemistry and Chemical Biology, Rutgers, The State University of New Jersey, New Brunswick, New Jersey 08854, United States*

Akshai Kumar − *Department of Chemistry, Indian Institute of Technology Guwahati, Guwahati – 781039, Assam, India*

Ashish Parihar − *Department of Chemistry and Chemical Biology, Rutgers, The State University of New Jersey, New Brunswick, New Jersey 08854, United States*

Thomas J. Emge − *Department of Chemistry and Chemical Biology, Rutgers, The State University of New Jersey, New Brunswick, New Jersey 08854, United States;* orcid.org/0000-0003-4685-8419

Complete contact information is available at: https://pubs.acs.org/10.1021/jacs.xxxxx

Notes

The authors declare no competing financial interests.

■ **ACKNOWLEDGMENTS**. This work was supported by the U. S. Department of Energy Office of Science (DE-SC0020139).

■ REFERENCES

(1) Moulton, C. J.; Shaw, B. L., Transition Metal-Carbon Bonds. Part XLII. Complexes of Nickel, Palladium, Platinum, Rhodium and Iridium with the Tridentate Ligand 2,6-bis[(di-tert-butylphosphino)methyl]phenyl. *J. Chem. Soc., Dalton Trans.* **1976**, 1020-1024. https://doi.org/10.1039/DT9760001020

(2) Fraser, P. J.; Roper, W. R.; Stone, F. G. A., Carbene complexes of iridium, rhodium, manganese, chromium, and iron containing thiazolidinylidene and pyridinylidene ligands. *J. Chem. Soc., Dalton Trans.* **1974**, 760-764. http://dx.doi.org/10.1039/DT9740000760

(3) Desguin, B.; Zhang, T.; Soumillion, P.; Hols, P.; Hu, J.; Hausinger, R. P., A tethered niacin-derived pincer complex with a nickel-carbon bond in lactate racemase. *Science* **2015,** *349*, 66-69. https://doi.org/10.1126/science.aab2272

(4) Xu, T.; Bauer, G.; Hu, X., A Novel Nickel Pincer Complex in the Active Site of Lactate Racemase. *ChemBioChem* **2016,** *17*, 31-32. https://doi.org/10.1002/cbic.201500498

(5) Schuster, O.; Yang, L.; Raubenheimer, H. G.; Albrecht, M., Beyond Conventional N-Heterocyclic Carbenes: Abnormal, Remote, and Other Classes of NHC Ligands with Reduced Heteroatom Stabilization. *Chem. Rev.* **2009,** *109*, 3445-3478. https://doi.org/10.1021/cr8005087

(6) Strasser, C. E.; Stander-Grobler, E.; Schuster, O.; Cronje, S.; Raubenheimer, H. G., Preparation of Remote NHC Complexes of Rhodium(I) and Gold(I) by Ligand Transfer. *Eur. J. Inorg. Chem.* **2009,** *2009*, 1905-1912. https://doi.org/10.1002/ejic.200801180

(7) Heydenrych, G.; von Hopffgarten, M.; Stander, E.; Schuster, O.; Raubenheimer, H. G.; Frenking, G., The Nature of the Metal–Carbene Bond in Normal and Abnormal Pyridylidene, Quinolylidene and Isoquinolylidene Complexes. *Eur. J. Inorg. Chem.* **2009,** *2009*, 1892-1904. https://doi.org/10.1002/ejic.200801244

(8) Alvarez, E.; Hernandez, Y. A.; Lopez-Serrano, J.; Maya, C.; Paneque, M.; Petronilho, A.; Poveda, M. L.; Salazar, V.; Vattier, F.; Carmona, E., Metallacyclic Pyridylidene Structures from Reactions of Terminal Pyridylidenes with Alkenes and Acetylene. *Angew. Chem., Intl. Ed.* **2010,** *49*, 3496-3499, S3496/3491-S3496/3438. https://doi.org/10.1002/anie.201000608

(9) Segarra, C.; Mas-Marza, E.; Mata, J. A.; Peris, E., Rhodium and Iridium Complexes with Chelating C-C '-Imidazolylidene-Pyridylidene Ligands: Systematic Approach to Normal, Abnormal, and Remote Coordination Modes. *Organometallics* **2012,** *31*, 5169-5176. https://doi.org/10.1021/om3005096

(10) Bajo, S.; Esteruelas, M. A.; Lopez, A. M.; Onate, E., Alkenylation of 2-methylpyridine via pyridylidene-osmium complexes. *Organometallics* **2012,** *31*, 8618-8626. https://doi.org/10.1021/om301058n

(11) Albrecht, M., Chapter Two - Normal and Abnormal N-Heterocyclic Carbene Ligands: Similarities and Differences of Mesoionic C–Donor Complexes. In *Adv. Organomet. Chem.*, Pérez, P. J., Ed. Academic Press: 2014; Vol. 62, pp 111-158. https://www.sciencedirect.com/science/article/pii/B9780128009765000023

(12) Vivancos, Á.; Segarra, C.; Albrecht, M., Mesoionic and Related Less Heteroatom-Stabilized N-Heterocyclic Carbene Complexes: Synthesis, Catalysis, and Other Applications. *Chem. Rev.* **2018,** *118*, 9493-9586. https://doi.org/10.1021/acs.chemrev.8b00148

(13) Schneider, S. K.; Julius, G. R.; Loschen, C.; Raubenheimer, H. G.; Frenking, G.; Herrmann, W. A., A first structural and theoretical comparison of pyridinylidene-type rNHC (remote N-heterocyclic carbene) and NHC complexes of Ni(ii) obtained by oxidative substitution. *Dalton Trans.* **2006**, 1226-1233. http://dx.doi.org/10.1039/B512419K

(14) Crociani, B.; Dibianca, F.; Bertani, R.; Castellani, C. B., Insertion of isocyanides into the palladium—carbon bond of C2-palladated heterocycles. Synthesis of trans-[PdCl{C(RN)=NR}(PPh_3)$_2$] complexes (RN = 2-pyridyl, 2-pyrazyl; R = alkyl or aryl group). *Inorg. Chim. Acta* **1985,** *101*, 161-169. https://doi.org/10.1016/S0020-1693(00)87650-1

(15) Crociani, B.; Di Bianca, F.; Giovenco, A.; Berton, A., N-protonated 2-pyridylnickel(II) complexes insertion of isocyanides into the nickel–2-pyridyl bond. *J. Organomet. Chem.* **1987,** *323*, 123-134. https://www.sciencedirect.com/science/article/pii/0022328X87871346

(16) Swisher, N. A.; Grubbs, R. H., Synthesis and Characterization of 3,5-Bis(di-tert-butylphosphinito)pyridine Pincer Complexes. *Organometallics* **2020,** *39*, 2479-2485. https://doi.org/10.1021/acs.organomet.0c00270

(17) Horak, K. T.; VanderVelde, D. G.; Agapie, T., Tuning of Metal Complex Electronics and Reactivity by Remote Lewis Acid Binding to π-Coordinated Pyridine Diphosphine Ligands. *Organometallics* **2015,** *34*, 4753-4765. https://doi.org/10.1021/acs.organomet.5b00562
(18) Tang, S.; von Wolff, N.; Diskin-Posner, Y.; Leitus, G.; Ben-David, Y.; Milstein, D., Pyridine-Based PCP-Ruthenium Complexes: Unusual Structures and Metal–Ligand Cooperation. *J. Am. Chem. Soc.* **2019,** *141*, 7554-7561. https://doi.org/10.1021/jacs.9b02669
(19) Zhang, X.; Chung, L. W., Alternative Mechanistic Strategy for Enzyme Catalysis in a Ni-Dependent Lactate Racemase (LarA): Intermediate Destabilization by the Cofactor. *Chem.-Eur. J.* **2017,** *23*, 3623-3630. https://doi.org/10.1002/chem.201604893
(20) Wang, B.; Shaik, S., The Nickel-Pincer Complex in Lactate Racemase Is an Electron Relay and Sink that acts through Proton-Coupled Electron Transfer. *Angew. Chem., Intl. Ed.* **2017,** *56*, 10098-10102. https://doi.org/10.1002/anie.201612065
(21) Xu, T.; Wodrich, M. D.; Scopelliti, R.; Corminboeuf, C.; Hu, X., Nickel pincer model of the active site of lactate racemase involves ligand participation in hydride transfer. *Proc. Natl. Acad. Sci.* **2017,** *114*, 1242-1245. https://doi.org/10.1073/pnas.1616038114
(22) Shi, R.; Wodrich, M. D.; Pan, H.-J.; Tirani, F. F.; Hu, X., Functional Models of the Nickel Pincer Nucleotide Cofactor of Lactate Racemase. *Angew. Chem., Intl. Ed.* **2019,** *58*, 16869-16872. https://doi.org/10.1002/anie.201910490
(23) Qiu, B.; Yang, X., A bio-inspired design and computational prediction of scorpion-like SCS nickel pincer complexes for lactate racemization. *Chem. Commun.* **2017,** *53*, 11410-11413. http://dx.doi.org/10.1039/C7CC06416K
(24) Rankin, J. A.; Mauban, R. C.; Fellner, M.; Desguin, B.; McCracken, J.; Hu, J.; Varganov, S. A.; Hausinger, R. P., Lactate Racemase Nickel-Pincer Cofactor Operates by a Proton-Coupled Hydride Transfer Mechanism. *Biochemistry* **2018,** *57*, 3244-3251. https://doi.org/10.1021/acs.biochem.8b00100
(25) Canovese, L.; Visentin, F.; Uguagliati, P.; Di Bianca, F.; Fontana, A.; Crociani, B., Organometallic nucleophiles. A mechanistic study of halide displacement at saturated carbon by 2- and 4-pyridyl complexes of palladium(II) and platinum(II). *J. Organomet. Chem.* **1996,** *525*, 43-48. https://doi.org/10.1016/S0022-328X(96)06490-X
(26) Canovese, L.; Uguagliati, P.; Di Bianca, F.; Crociani, B., Organometallic nucleophiles. Mechanism of halide displacement at saturated carbon by 2-pyridyl and 4-Pyridyl complexes [M(dmtc)(C_5H_4N-Cn)(L)] (M = Pd, Pt; dmtc = dimethyldithiocarbamate; n = 2,4; L = tertiary phosphine. *J. Organomet. Chem.* **1992,** *438*, 253-263. https://doi.org/10.1016/0022-328X(92)88023-C
(27) Crociani, B.; Di Bianca, F.; Uguagliati, P.; Canovese, L., A powerful organometallic nucleophile the 2-pyridyl group in (dimethyldithio-carbamate) (2-pyridyl)(triphenyl-phosphine)platinum(II). *Inorg. Chim. Acta* **1990,** *176*, 5-6. https://doi.org/10.1016/S0020-1693(00)85080-X
(28) Crociani, B.; di Bianca, F.; Giovenco, A.; Scrivanti, A., Protonation and methylation reactions of 2-pyridyl-palladium(II) and -platinum(II) complexes. *J. Organomet. Chem.* **1983,** *251*, 393-411. https://www.sciencedirect.com/science/article/pii/S0022328X00987850
(29) Kuo, J. L.; Goldberg, K. I., Metal/Ligand Proton Tautomerism Facilitates Dinuclear H2 Reductive Elimination. *J. Am. Chem. Soc.* **2020,** *142*, 21439-21449. https://doi.org/10.1021/jacs.0c10458
(30) Jain, A. K.; Gau, M. R.; Carroll, P. J.; Goldberg, K. I., Comparing Square-Planar Rh^{I} and Ir^{I}: Metal–Ligand Proton Tautomerism, Fluxionality, and Reactivity. *Organometallics* **2022,** *41*, 3341–3348. https://doi.org/10.1021/acs.organomet.2c00302
(31) Jain, A. K.; Gau, M. R.; Carroll, P. J.; Goldberg, K. I., The underappreciated influence of ancillary halide on metal–ligand proton tautomerism. *Chem. Sci.* **2022,** *13*, 7837-7845. http://dx.doi.org/10.1039/D2SC00279E
(32) Esteruelas, M. A.; Fernández-Alvarez, F. J.; Oñate, E., Stabilization of NH Tautomers of Quinolines by Osmium and Ruthenium. *J. Am. Chem. Soc.* **2006,** *128*, 13044-13045. https://doi.org/10.1021/ja064979l
(33) Esteruelas, M. A.; Fernández-Alvarez, F. J.; Oñate, E., Osmium and Ruthenium Complexes Containing an N-Heterocyclic Carbene Ligand Derived from Benzo[h]quinoline. *Organometallics* **2007,** *26*, 5239-5245. https://doi.org/10.1021/om700639a

(34) Esteruelas, M. A.; Fernandez-Alvarez, F. J.; Olivan, M.; Onate, E., NH-Tautomerization of Quinolines and 2-Methylpyridine Promoted by a Hydride-Iridium(III) Complex: Importance of the Hydride Ligand. *Organometallics* **2009,** *28*, 2276-2284. https://doi.org/10.1021/om8011954
(35) Buil, M. L.; Esteruelas, M. A.; Garces, K.; Olivan, M.; Onate, E., C_{beta} (sp^2)-H Bond Activation of alpha, beta -Unsaturated Ketones Promoted by a Hydride-Elongated Dihydrogen Complex: Formation of Osmafuran Derivatives with Carbene, Carbyne, and NH-Tautomerized alpha -Substituted Pyridine Ligands. *Organometallics* **2008,** *27*, 4680-4690. https://doi.org/10.1021/om800439g
(36) Wiedemann, S. H.; Lewis, J. C.; Ellman, J. A.; Bergman, R. G., Experimental and Computational Studies on the Mechanism of N-Heterocycle C-H Activation by Rh(I). *J. Am. Chem. Soc.* **2006,** *128*, 2452-2462. https://doi.org/10.1021/ja0576684
(37) Lewis, J. C.; Berman, A. M.; Bergman, R. G.; Ellman, J. A., Rh(I)-Catalyzed Arylation of Heterocycles via C-H Bond Activation: Expanded Scope through Mechanistic Insight. *J. Am. Chem. Soc.* **2008,** *130*, 2493-2500. https://doi.org/10.1021/ja0748985
(38) Lewis, J. C.; Bergman, R. G.; Ellman, J. A., Rh(I)-Catalyzed Alkylation of Quinolines and Pyridines via C-H Bond Activation. *J. Am. Chem. Soc.* **2007,** *129*, 5332-5333. https://doi.org/10.1021/ja070388z
(39) Joule, J. A.; Mills, K., Pyridines: Reactions and Synthesis. In *Heterocyclic Chemistry*, 5th ed.; John Wiley & Sons: West Sussex, UK, 2010; pp 158-162.
(40) Punji, B.; Emge, T. J.; Goldman, A. S., A Highly Stable Adamantyl-Substituted Pincer-Ligated Iridium Catalyst for Alkane Dehydrogenation. *Organometallics* **2010,** *29*, 2702-2709. http://dx.doi.org/10.1021/om100145q
(41) Grimm, J. C.; Nachtigal, C.; Mack, H. G.; Kaska, W. C.; Mayer, H. A., A novel functionalized P,C,P pincer ligand complex. *Inorg. Chem. Comm.* **2000,** *3*, 511-514. https://doi.org/10.1016/S1387-7003(00)00132-5
(42) Mohammad, H. A. Y.; Grimm, J. C.; Eichele, K.; Mack, H.-G.; Speiser, B.; Novak, F.; Quintanilla, M. G.; Kaska, W. C.; Mayer, H. A., C-H Oxidative Addition with a (PCP)Ir(III)-Pincer Complex. *Organometallics* **2002,** *21*, 5775-5784. http://dx.doi.org/10.1021/om020621w
(43) Huang, Z.; Brookhart, M.; Goldman, A. S.; Kundu, S.; Ray, A.; Scott, S. L.; Vicente, B. C., Highly Active and Recyclable Heterogeneous Iridium Pincer Catalysts for Transfer Dehydrogenation of Alkanes. *Adv. Synth. Catal.* **2009,** *351*, 188-206. http://dx.doi.org/10.1002/adsc.200800615
(44) Kütt, A.; Selberg, S.; Kaljurand, I.; Tshepelevitsh, S.; Heering, A.; Darnell, A.; Kaupmees, K.; Piirsalu, M.; Leito, I., pKa values in organic chemistry – Making maximum use of the available data. *Tetrahedron Lett.* **2018,** *59*, 3738-3748. https://www.sciencedirect.com/science/article/pii/S0040403918310554
(45) Kundu, S.; Choi, J.; Wang, D. Y.; Choliy, Y.; Emge, T. J.; Krogh-Jespersen, K.; Goldman, A. S., Cleavage of Ether, Ester, and Tosylate C(sp^3)-O Bonds by an Iridium Complex, Initiated by Oxidative Addition of C-H Bonds. Experimental and Computational Studies. *J. Am. Chem. Soc.* **2013,** *135*, 5127-5143. http://dx.doi.org/10.1021/ja312464b
(46) Lokare, K. S.; Nielsen, R. J.; Yousufuddin, M.; Goddard Iii, W. A.; Periana, R. A., Iridium complexes bearing a PNP ligand, favoring facile C(sp3)–H bond cleavage. *Dalton Trans.* **2011,** *40*, 9094-9097. http://dx.doi.org/10.1039/C1DT10577A
(47) Isobe, K.; Nakamura, Y.; Miwa, T.; Kawaguchi, S., Comparative Studies of 2-, 3-, and 4-Pyridylpalladium(II) Complexes: Synthesis and Properties. *Bull. Chem. Soc. Jpn.* **1987,** *60*, 149-157. https://doi.org/10.1246/bcsj.60.149
(48) Polukeev, A. V.; Kuklin, S. A.; Petrovskii, P. V.; Peregudov, A. S.; Dolgushin, F. M.; Ezernitskaya, M. G.; Koridze, A. A., Reactions of iridium bis(phosphinite) pincer complexes with protic acids. *Russ. Chem. Bull.* **2010,** *59*, 745-749. https://doi.org/10.1007/s11172-010-0156-6
(49) Conner, D.; Jayaprakash, K. N.; Cundari, T. R.; Gunnoe, T. B., Synthesis and Reactivity of a Coordinatively Unsaturated Ruthenium(II) Parent Amido Complex: Studies of X-H Activation (X = H or C). *Organometallics* **2004,** *23*, 2724-2733. https://doi.org/10.1021/om049836r
(50) Connelly, N. G.; Geiger, W. E., Chemical Redox Agents for Organometallic Chemistry. *Chem. Rev.* **1996,** *96*, 877-910. http://dx.doi.org/10.1021/cr940053x
(51) Warren, J. J.; Tronic, T. A.; Mayer, J. M., Thermochemistry of Proton-Coupled Electron Transfer Reagents and its Implications. *Chem. Rev.* **2010,** *110*, 6961-7001. http://pubs.acs.org/doi/abs/10.1021/cr100085k

(52) Mader, E. A.; Manner, V. W.; Markle, T. F.; Wu, A.; Franz, J. A.; Mayer, J. M., Trends in Ground-State Entropies for Transition Metal Based Hydrogen Atom Transfer Reactions. *J. Am. Chem. Soc.* **2009,** *131*, 4335-4345. https://doi.org/10.1021/ja8081846
(53) Manner, V. W.; Markle, T. F.; Freudenthal, J. H.; Roth, J. P.; Mayer, J. M., The first crystal structure of a monomeric phenoxyl radical: 2,4,6-tri-tert-butylphenoxyl radical. *Chem. Commun.* **2008**, 256-258. http://dx.doi.org/10.1039/B712872J
(54) Morris, R. H., Estimating the Acidity of Transition Metal Hydride and Dihydrogen Complexes by Adding Ligand Acidity Constants. *J. Am. Chem. Soc.* **2014,** *136*, 1948-1959. https://doi.org/10.1021/ja410718r
(55) Curtis, C. J.; Miedaner, A.; Ciancanelli, R.; Ellis, W. W.; Noll, B. C.; Rakowski DuBois, M.; DuBois, D. L., $[Ni(Et_2PCH_2NMeCH_2PEt_2)_2]_2^+$ as a Functional Model for Hydrogenases. *Inorg. Chem.* **2003,** *42*, 216-227. https://doi.org/10.1021/ic020610v
(56) Brookhart, M.; Green, M. L. H.; Parkin, G., Agostic Interactions in Transition Metal Compounds. *Proc. Natl. Acad. Sci.* **2007,** *104*, 6908-6914. https://doi.org/10.1073/pnas.0610747104
(57) Hebden, T. J.; Schrock, R. R.; Takase, M. K.; Muller, P., Cleavage of dinitrogen to yield a (t-BuPOCOP)molybdenum(IV) nitride. *Chem. Commun.* **2012,** *48*, 1851-1853. http://dx.doi.org/10.1039/C2CC17634C
(58) Leoni, P.; Pasquali, M.; Sommovigo, M.; Laschi, F.; Zanello, P.; Albinati, A.; Lianza, F.; Pregosin, P. S.; Rueegger, H., Chemistry of phosphido-bridged palladium(I) dimers. .eta.2-Pd-H-P interactions: a new bonding mode for secondary phosphines. *Organometallics* **1993,** *12*, 1702-1713. https://doi.org/10.1021/om00029a031
(59) Albinati, A.; Lianza, F.; Pasquali, M.; Sommovigo, M.; Leoni, P.; Pregosin, P. S.; Ruegger, H., Palladium-hydrogen-phosphorus bridging in a palladium(I) dimer. *Inorg. Chem.* **1991,** *30*, 4690-4692. https://doi.org/10.1021/ic00025a004
(60) Williams, D. B.; Kaminsky, W.; Mayer, J. M.; Goldberg, K. I., Reactions of iridium hydride pincer complexes with dioxygen: new dioxygen complexes and reversible O_2 binding. *Chem. Commun.* **2008**, 4195-4197. https://doi.org/10.1039/B802739K
(61) Alvarez, E.; Conejero, S.; Paneque, M.; Petronilho, A.; Poveda, M. L.; Serrano, O.; Carmona, E., Iridium(III)-Induced Isomerization of 2-Substituted Pyridines to N-Heterocyclic Carbenes. *J. Am. Chem. Soc.* **2006,** *128*, 13060-13061. https://doi.org/10.1021/ja0646592
(62) Álvarez, E.; Conejero, S.; Lara, P.; López, J. A.; Paneque, M.; Petronilho, A.; Poveda, M. L.; del Río, D.; Serrano, O.; Carmona, E., Rearrangement of Pyridine to Its 2-Carbene Tautomer Mediated by Iridium. *J. Am. Chem. Soc.* **2007,** *129*, 14130-14131. https://doi.org/10.1021/ja075685i
(63) Mohammad, H. A. Y.; Grimm, J. C.; Eichele, K.; Mack, H.-G.; Speiser, B.; Novak, F.; Kaska, W. C.; Mayer, H. A., Double cyclometalation: Implications for C-H oxidative addition with PCP pincer compounds of iridium. *ACS Symposium Series* **2004,** *885*, 234-247. https://doi.org/10.1021/bk-2004-0885.ch014
(64) Novak, F.; Speiser, B.; Mohammad, H. A. Y.; Mayer, H. A., Electrochemistry of transition metal complex catalysts: Part 10. Intra- and intermolecular electrochemically activated C-H addition to the central metal atom of a P–C–P-pincer iridium complex. *Electrochim. Acta* **2004,** *49*, 3841-3853. https://doi.org/10.1016/j.electacta.2003.11.038
(65) Das, K.; Kumar, A., Alkane dehydrogenation reactions catalyzed by pincer-metal complexes. *Adv. Organomet. Chem.* **2019,** *72*, 1-57. https://doi.org/10.1016/bs.adomc.2019.02.0041
(66) Kumar, A.; Bhatti, T. M.; Goldman, A. S., Dehydrogenation of Alkanes and Aliphatic Groups by Pincer-Ligated Metal Complexes. *Chem. Rev.* **2017,** *117*, 12357-12384. http://dx.doi.org/10.1021/acs.chemrev.7b00247
(67) Fang, H.; Liu, G.; Huang, Z., Pincer iridium and ruthenium complexes for alkane dehydrogenation. In *Pincer Compounds Chemistry and Applications*, Morales-Morales, D., Ed. Elsevier B.V.: Amsterdam, 2018; pp 383-399. https://www.sciencedirect.com/science/book/9780128129319
(68) Gordon, B. M.; Lease, N.; Emge, T. J.; Hasanayn, F.; Goldman, A. S., Reactivity of Iridium Complexes of a Triphosphorus-Pincer Ligand Based on a Secondary Phosphine. Catalytic Alkane Dehydrogenation and the Origin of Extremely High Activity. *J. Am. Chem. Soc.* **2022,** *144*, 4133-4146. https://doi.org/10.1021/jacs.1c13309

(69) Reamey, R. H.; Whitesides, G. M., Mechanism of hydrogenolysis of dineopentylbis(triethylphosphine)platinum(II). *J. Am. Chem. Soc.* **1984,** *106*, 81-85. https://doi.org/10.1021/ja00313a018
(70) Jones, W. D.; Feher, F. J., Kinetics and thermodynamics of intra- and intermolecular carbon-hydrogen bond activation. *J. Am. Chem. Soc.* **1985,** *107*, 620-631. https://pubs.acs.org/doi/pdf/10.1021/ja00289a014
(71) To capture the low entropic penalty associated with the addition of an alkane molecule in alkane solvent or at a very high concentration of alkane, the reaction was calculated with a van der Waals complex of the metal complex and alkane molecule as the reactant, rather than free metal complex and a gas-phase alkane molecule. See reference 72.
(72) Zhou, X.; Malakar, S.; Dugan, T.; Wang, K.; Sattler, A.; Marler, D. O.; Emge, T. J.; Krogh-Jespersen, K.; Goldman, A. S., Alkane Dehydrogenation Catalyzed by a Fluorinated Phebox Iridium Complex. *ACS Catal.* **2021,** *11*, 14194-14209. https://doi.org/10.1021/acscatal.1c03562
(73) Smidt, J.; Hafner, W.; Jira, R.; Sedlmeier, J.; Sieber, R.; Rüttinger, R.; Kojer, H., Katalytische Umsetzungen von Olefinen an Platinmetall-Verbindungen Das Consortium-Verfahren zur Herstellung von Acetaldehyd. *Angew. Chem.* **1959,** *71*, 176-182. https://doi.org/10.1002/ange.19590710503
(74) Shada, A. D. R.; Miller, A. J. M.; Emge, T. J.; Goldman, A. S., Catalytic Dehydrogenation of Alkanes by PCP–Pincer Iridium Complexes Using Proton and Electron Acceptors. *ACS Catal.* **2021,** *11*, 3009-3016. https://doi.org/10.1021/acscatal.0c05160